

Signatures for Short-Range Correlations in ^{16}O Observed in the Reaction $^{16}\text{O}(e, e'pp)^{14}\text{C}$

C. J. G. Onderwater,^{1,2,*} K. Allaart,¹ E. C. Aschenauer,^{2,†} Th. S. Bauer,^{2,4} D. J. Boersma,^{2,4} E. Cisbani,³ W. H. Dickhoff,⁵ S. Frullani,³ F. Garibaldi,³ W. J. W. Geurts,¹ C. Giusti,⁶ D. L. Groep,² W. H. A. Hesselink,^{1,2} M. Iodice,³ E. Jans,² N. Kalantar-Nayestanaki,⁷ W.-J. Kasdorp,² C. Kormanyos,^{1,2} L. Lapidás,² J. J. van Leeuwe,² R. De Leo,⁸ A. Misiejuk,^{2,4} H. Müther,⁹ F. D. Pacati,⁶ A. R. Pellegrino,^{1,2,†} R. Perrino,⁸ R. Starink,^{1,2} M. Steenbakkens,^{1,2} G. van der Steenhoven,² J. J. M. Steijger,² M. A. van Uden,² G. M. Urciuoli,³ L. B. Weinstein,¹⁰ and H. W. Willering^{2,4}

¹*Department of Physics and Astronomy, Free University, de Boelelaan 1081, 1081 HV Amsterdam, The Netherlands*

²*NIKHEF, P.O. Box 41882, 1009 DB Amsterdam, The Netherlands*

³*Istituto Superiore di Sanità, Laboratorio di Fisica, INFN, Viale Regina Elena 299, Rome, Italy*

⁴*Universiteit Utrecht, P.O. Box 80.000, 3508 TA Utrecht, The Netherlands*

⁵*Department of Physics, Washington University, St. Louis, Missouri 63130*

⁶*Dipartimento di Fisica Nucleare e Teorica dell'Università, Pavia and INFN, Sezione di Pavia, Italy*

⁷*KVI, Rijksuniversiteit Groningen, Zernikelaan 25, 9747 AA Groningen, The Netherlands*

⁸*INFN Sezione di Lecce, via per Arnesano, 73100 Lecce, Italy*

⁹*Institut für Theoretische Physik, Universität Tübingen, Auf der Morgenstelle 14, D 72076, Tübingen, Germany*

¹⁰*Department of Physics, Old Dominion University, Norfolk, Virginia 23529*

(Received 23 April 1998)

The reaction $^{16}\text{O}(e, e'pp)^{14}\text{C}$ has been studied at a transferred four-momentum $(\omega, |\mathbf{q}|) = (210 \text{ MeV}, 300 \text{ MeV}/c)$. The differential cross sections for the transitions to the ground state and the lowest excited states in ^{14}C were determined as a function of the momentum of the recoiling ^{14}C nucleus and the angle between the momentum of the proton emitted in the forward direction and the momentum transfer \mathbf{q} . A comparison of the data to the results of calculations, performed with a microscopic model, shows clear signatures for short-range correlations in the ^{16}O ground state. [S0031-9007(98)07083-5]

PACS numbers: 21.10.Pc, 21.30.Fe, 25.30.Fj, 27.20.+n

In recent years, studies on short-range correlations (SRC) in nuclei have made striking progress. Microscopic many-body calculations in nuclear matter [1–3] and nuclei [4–6] have shown that SRC can account for a sizable fraction of the depletion in the occupancy of the valence orbits, observed in $(e, e'p)$ proton knockout reactions [7]. Furthermore, these calculations predict an enhancement of the high-momentum components in the nucleon wave functions. Signatures of admixtures of high-momentum components in the nuclear ground state are expected to be found in the $(e, e'p)$ reaction at high missing energies and in two-nucleon knockout $(e, e'NN)$ studies [8,9]. Although experimentally more involved, the latter reactions have distinct advantages as a probe for studying SRC in nuclei.

In an exclusive $(e, e'NN)$ reaction both ejectiles are identified and the excitation energy of the residual nucleus is determined by energy conservation. This allows the measurement of the cross section for transitions to discrete states, as has recently been shown for the $^{16}\text{O}(e, e'pp)^{14}\text{C}$ reaction [10,11]. Furthermore, the reaction mechanism for two-nucleon knockout by virtual photons depends on the spin and isospin of the nucleon pair in the initial state. This implies that complementary information on SRC can be extracted from $(e, e'pp)$ and $(e, e'pn)$ reaction studies.

In Ref. [10], we have presented the first results of a triple coincidence $^{16}\text{O}(e, e'pp)^{14}\text{C}$ experiment. The excitation

energy spectrum up to 20 MeV of the residual nucleus ^{14}C and the corresponding missing-momentum distributions were compared with calculations performed within a simple factorization approximation of the cross section. In this Letter the differential cross sections are presented as a function of the excitation energy, the missing momentum, and the emission angle of the forward proton. The data are compared to the results of calculations performed with the microscopic model, recently described in Ref. [9].

The measurements were performed with the high duty-factor electron beam extracted from the pulse-stretcher AmPS at NIKHEF. The measurements were performed with 584 MeV electrons and the scattered electrons were detected at an angle of 26° . The central values of the energy transfer ω and three-momentum transfer $|\mathbf{q}|$ were 210 MeV and 300 MeV/c, respectively. Protons, with momenta \mathbf{p}_1 and \mathbf{p}_2 , were detected at angles in the range 8° – 40° and 115° – 155° with respect to \mathbf{q} . The proton energy acceptances were 70–220 MeV and 44–178 MeV, respectively. Details of the beam, the target, the experimental setup and the first stage of the analysis can be found in Ref. [10].

In order to present absolute cross sections, special attention was paid to the calibration of the experimental equipment. For this purpose, the data were corrected on an event-by-event basis for inefficiencies in the detectors, the electronic readout and data-acquisition systems, and in

the determination of proton events. The most important corrections are those for the dead times of the frontend electronics and trigger system, multiple hits in the first layers of the proton detectors, and multiple-scattering and hadronic interactions in these detectors. The dead times of the frontends were determined using a laser/testpulse system. The corrections made for hadronic interactions and multiple scattering effects in the proton detectors result from simulations of the detector response performed with the GEANT Monte-Carlo code [12].

The ninefold-differential cross sections were obtained by subtracting the contribution of accidental coincidences and by normalizing the corrected yields to the total luminosity and the detection volume. The cross sections are presented as a function of three variables: the excitation energy E_x of the final nucleus ^{14}C , the missing momentum p_m , defined as $|\mathbf{p}_m| = |\mathbf{q} - \mathbf{p}_1 - \mathbf{p}_2|$, and the angle γ_1 between the momentum of the proton emitted in the forward direction and the transferred momentum \mathbf{q} . For a particular state, the p_m distribution is characterized by the angular momentum of the center-of-mass motion of the knocked out proton pair in the initial state, which in turn is linked, by angular momentum conservation, to the angular momentum associated to the relative motion of the two protons in the initial state. Hence, one may expect that the p_m distribution will reflect the contributions of the various partial waves for the relative motion, notably those for the 1S_0 and 3P waves [10]. The dependence of the cross sections on γ_1 is expected to provide information on the reaction mechanism, since calculations indicate that the contributions of one- and two-body currents to the cross section exhibit a different trend as a function of γ_1 .

The E_x distribution was corrected for the effects due to radiation processes, in a way similar to that for (e, e') data. It was argued in Ref. [13] that an unfolding procedure for more than one variable in an $(e, e'pp)$ reaction, which is extremely complicated, is not always needed. In the present experiment, the effects of omitting the unfolding of the cross sections as a function of p_m and γ_1 is negligible in view of the resolution of the distributions in these variables, which are 7 MeV/c and 0.8° , respectively. Note that the corrections made for the E_x spectrum are also accounted for in the p_m and γ_1 distributions for selected regions in E_x .

The total systematic error in the cross sections, which is $(-6\%, +16\%)$ is mainly determined by the uncertainty in the integrated luminosity (3%), the uncertainty in the correction for hadronic interactions and multiple scattering effects (5%), and the uncertainty in the determination of the electronics live times (+10%).

The cross sections as a function of each of the variables E_x , p_m , and γ_1 were obtained by summing the cross sections for selected bins in the other two variables (weighted with $\sin \gamma_1$ to account for the phase space) and by dividing the resulting sum by the (weighted) number of bins.

In Fig. 1 the differential cross sections, averaged over the p_m range from 50 to 350 MeV/c and the γ_1 range from 10° to 40° , are shown as a function of the excitation energy. The five lowest-lying states that are expected to be excited in the $^{16}\text{O}(e, e'pp)^{14}\text{C}$ reaction are indicated by their values J^π . As argued in Ref. [10], their excitation energies were partly taken from previous experiments and partly estimated on the basis of calculations.

The experimental energy resolution of 3.9 MeV FWHM does not allow the separation of the individual states, except the ground state. Consequently, the eightfold-differential cross section for the transition to a particular state cannot be determined exclusively. Instead, the ninefold-differential cross section was integrated over three, suitably chosen, intervals of the excitation energy. The first interval ranges from -4 to 4 MeV and contains almost exclusively the strength of the ground-state transition. The strength in the E_x interval from 4 to 9 MeV can be assigned predominantly to the excitation of the 2_1^+ state, of which the centroid excitation energy is 7.7 MeV. The contribution of the next state ($J^\pi = 1^+$, $E_x = 11.3$ MeV) to this interval is small. Finally, the strength in the interval from 9 to 14 MeV can be attributed to the excitation of the 1^+ and 0_2^+ (estimated energy $E_x = 12$ MeV) states. Because of the increasing strength of the continuum, which stems from multinucleon emission and the knockout of one or both emitted protons from the $1s$ shell, it is difficult to extract accurate information on the $(e, e'pp)$ process from the data for $E_x \geq 14$ MeV. Therefore, only the cross section distributions for the three bins mentioned above are considered and presented in Fig. 2 as a function of p_m and γ_1 .

It should be noted that the recoil factor, $\partial E_2/\partial E_x$, in the expression of the eightfold-differential cross section has not been taken into account. This factor cannot be

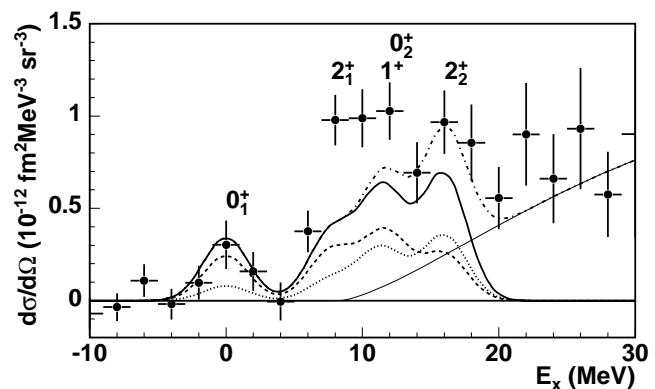


FIG. 1. The ninefold-differential cross section as a function of the excitation energy, averaged over missing momenta between 50 and 350 MeV/c and over γ_1 between 10° and 40° ($d\sigma/d\Omega = d^9\sigma/dE_{e'}d\Omega_{e'}dE_1d\Omega_1dE_2d\Omega_2$). The measured cross sections are indicated with the solid circles. The error bars represent the statistical uncertainty. The curves correspond to results of a microscopic calculation (see text).

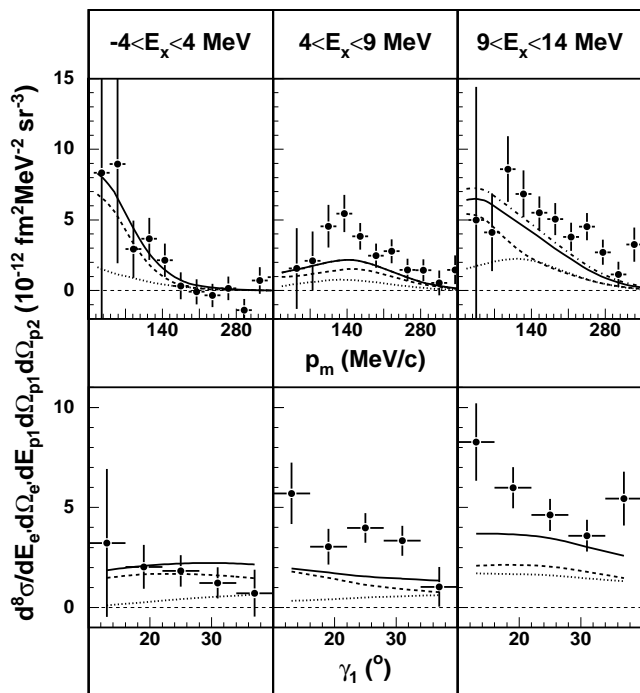


FIG. 2. The eightfold-differential cross section integrated over the indicated excitation-energy ranges. The upper panels show the cross sections as a function of p_m averaged over the γ_1 range from 10° to 40° . The lower panels show the cross sections as a function of γ_1 averaged over the p_m ranges from 45, 60, and 70 to 300 MeV/c, for the three consecutive bins in E_x . The curves correspond to the same calculations as in Fig. 1.

expressed uniquely in the variables E_x , p_m , and γ_1 but depends on the momenta of the emitted protons. However, for the present kinematical conditions the recoil factor is always close to unity and has only a minor effect on the cross sections.

The curves in Figs. 1 and 2 are the results of recent microscopic calculations of the differential cross sections for transitions to discrete states in the residual ^{14}C nucleus [9]. To allow a comparison with the data, the theoretical cross sections were folded with a Gaussian distribution to account for the experimental energy resolution and integrated over the same energy intervals as the experimental ones.

In the calculations, the transition amplitude for the $(e, e'pp)$ reaction contains contributions of one-body hadronic currents, which are related to the direct knockout of two correlated nucleons, as well as those of two-body currents, which involve the intermediate excitation of the Δ isobar. The interaction of the outgoing protons with the residual nucleus is treated in terms of an optical potential. The two-proton spectral function for ^{16}O , needed to calculate the two-proton overlap integral in the transition amplitude, was obtained from dressed random-phase approximation (DRPA) calculations [14], which were performed in a harmonic oscillator (HO) basis within a large configuration space to account for the effects of

long-range correlations. Short-range correlations were incorporated in the relative part of the wave functions of the proton pair by means of state-dependent defect functions [15], which were calculated using the realistic Bonn-A nucleon-nucleon potential.

In contrast to Ref. [9], where the HO wave functions for the bound states were calculated using an oscillator length $b = 1.77$ fm, we have taken $b = 2.0$ fm in the present calculations. With the latter value one obtains a better description of the quasihole wave functions calculated in Ref. [6] for the $l = 1$ states in ^{16}O in the momentum range 50–150 MeV/c, where they exhibit their maxima. The larger b value is required to simulate the effect of correlations in the wave functions presented in Ref. [6], which go beyond the limited configuration space employed in the DRPA calculations [14]. The HO wave function calculated with $b = 2.0$ fm was also found to give the best representation of the reduced cross sections for the ground-state transition in the $^{16}\text{O}(e, e'p)^{15}\text{N}$ reaction in the relevant momentum range [16].

In both figures, the theoretical cross sections for the knockout of two protons, predominantly from the $1p$ shell, are represented by the solid curves. The contributions of the one- and two-body nuclear currents are given by the dashed and dotted curves, respectively. To these theoretical results a continuum accounting for the emission of one or both protons from the $1s$ shell and for the emission of three nucleons is added (thin line in Fig. 1). The shape of the continuum has been determined by extrapolating a fit to the data, made in the region $25 \leq E_x \leq 70$ MeV, to the three-nucleon knockout threshold at $E_x = 8.3$ MeV. The dot-dashed curves in Figs. 1 and 2 correspond to the sum of the theoretical cross section and the continuum.

The calculated cross sections of Fig. 1 appear to agree surprisingly well with the data, given the fact that no parameter has been adjusted to fit the data with the exception of the continuum. Especially the cross section for the ground-state transition, which is separated from the other transitions, is well reproduced by the calculations. However, the strength in the part of the E_x spectrum that predominantly stems from the excitation of the 2_1^+ state ($4 < E_x < 9$ MeV) is underestimated by the calculations. To a lesser extent this also holds for the region where the strength for the transitions to the 1^+ and 0_2^+ resides ($9 < E_x < 14$ MeV).

The missing momentum distributions for various excitation-energy intervals (cf. Fig. 2) are described quite well by the calculations, both in shape and in amplitude. The shapes of the experimental as well as of the calculated distributions for the three regions in excitation energy nicely reflect the characteristic features of the orbital angular momenta associated with the center-of-mass motion of the proton pair in the initial state. This angular momentum is either $L = 0$ or $L = 1$ for the transitions to the ground state and 0_2^+ state, $L = 1$ or $L = 2$ for the

transitions to the 2^+ states, and $L = 1$ for the excitation of the 1^+ state. The center-of-mass angular momenta $L = 0$ and $L = 2$ are always associated with a 1S_0 wave for the relative motion and $L = 1$ always with a 3P wave (the minor contribution of the 1D_2 wave to the transition to the 2^+ states is not considered here). According to the calculations, knockout of a 1S_0 proton pair is mainly induced by the one-body current. Moreover, this part of the transition amplitude solely originates from SRC. Hence, the observation that the missing momentum distribution for the ground-state transition has its maximum at $p_m = 0$ MeV/c leads to the conclusion that this cross section is dominated by knockout of 1S_0 proton pairs and that, according to the calculations, this process is driven by SRC. Furthermore, the calculations predict that the contribution of one-body currents to the cross section is also dominant for the excitation of the 2_1^+ and 0_2^+ states, whereas the transition to the 1^+ state, which resides in the interval $9 < E_x < 14$ MeV, is largely driven by knockout of 3P pairs via two-body (Δ) currents. Though less significant than for the ground-state transition, this picture is also reflected in the shape of the experimental p_m distributions. Hence, these distributions already contain a strong indication that there is substantial contribution of two-proton knockout driven by one-body currents, which are determined by SRC.

Further evidence for the importance of SRC in the $^{16}\text{O}(e, e'pp)^{14}\text{C}$ reaction is obtained from the dependence of the cross section on the proton emission angle γ_1 shown in the lower panels of Fig. 2. The global trend is a gradual decrease of the cross sections as a function of γ_1 , whereas the theoretical results show a less pronounced γ_1 dependence. A comparison of the data with the contributions due to one-body and two-body currents separately indicates that the γ_1 dependence of the part of the cross section due to two-body currents deviates from the slope of the experimental data. On the other hand, the part of the cross section generated by the one-body currents is more in accordance with the data. At this point it is of interest to note that the range of relative momenta of two protons in the initial state probed in the $(e, e'pp)$ reaction depends on γ_1 . Assuming that the virtual photon is absorbed by the proton emitted in the forward direction, the angular dependence of the one-body part of the cross section directly reflects the distribution of the relative momentum of the strongly correlated protons.

In conclusion, the $^{16}\text{O}(e, e'pp)$ reaction has been studied at an energy transfer $\omega = 210$ MeV and a three-momentum transfer $|\mathbf{q}| = 300$ MeV/c. The cross sections measured as a function of the excitation energy up to 20 MeV are in satisfactory agreement with the results of calculations performed with a parameter-free microscopic model. Also the cross sections measured as a

function of the missing momentum and integrated over the three selected intervals in excitation energy are reproduced quite well by the calculations. Because the calculations show that the major contributions to the cross sections for the transitions to the ground state and the 2_1^+ state stem from the one-body currents, which are driven by SRC, it can be concluded that the data give clear indications for SRC in the ground state of ^{16}O . The deviations observed between the measured and the predicted dependences of the cross section on the emission angle of the forward proton suggest that the contribution of SRC to the reaction amplitude is underestimated by the calculations.

This work is part of the research programme of the "Stichting voor Fundamenteel Onderzoek der Materie (FOM)," which is financially supported by the "Nederlandse Organisatie voor Wetenschappelijk Onderzoek (NWO)." Additional support is provided by NSF Grant No. PHY-9602127.

*Present address: University of Illinois at Urbana-Champaign, 1110 West Green Street, Urbana, IL 61801-3080.

†Present address: Deutsche Elektronen-Synchrotron DESY, Notkestraße 85, D-22603 Hamburg, Germany.

- [1] O. Benhar, A. Fabrocini, and S. Fantoni, Nucl. Phys. **A505**, 267 (1989).
- [2] A. Ramos, A. Polls, and W.H. Dickhoff, Nucl. Phys. **A503**, 1 (1989).
- [3] B.E. Vonderfecht, W.H. Dickhoff, A. Polls, and A. Ramos, Nucl. Phys. **A555**, 1 (1993).
- [4] S.C. Pieper, R.B. Wiringa, and V.R. Pandharipande, Phys. Rev. C **46**, 1741 (1992).
- [5] H. Mütter and W.H. Dickhoff, Phys. Rev. C **49**, R17 (1994).
- [6] A. Polls *et al.*, Phys. Rev. C **55**, 810 (1997).
- [7] L. Lapidás, Nucl. Phys. **A553**, 297c (1993).
- [8] J. Ryckebusch *et al.*, Nucl. Phys. **A624**, 581 (1997).
- [9] C. Giusti *et al.*, Phys. Rev. C **57**, 1691 (1998).
- [10] C.J.G. Onderwater *et al.*, Phys. Rev. Lett. **78**, 4893 (1997).
- [11] G. Rosner, in *Proceedings of the Conference on Perspectives in Hadronic Physics*, edited by S. Boffi, C. Ciofi degli Atti, and M.M. Giannini (ICTP, World Scientific, Singapore, 1997), p. 1.
- [12] *GEANT: Detector Description and Simulation Tool*. CERN Program Library W5013, 1993.
- [13] L.J.H.M. Kester *et al.*, Phys. Lett. B **344**, 79 (1995).
- [14] W.J.W. Geurts, K. Allaart, W.H. Dickhoff, and H. Mütter, Phys. Rev. C **54**, 1144 (1996).
- [15] H. Mütter and P.U. Sauer, in *Computational Nuclear Physics*, edited by K.-H. Langanke, J.A. Maruhn, and S.E. Koonin (Springer, New York, 1993), p. 30.
- [16] M. Leuschner *et al.*, Phys. Rev. C **49**, 955 (1994).